

# Synthesis, Characterization and Photoluminescence Studies of near-UV excitable green-emitting NaBaScSi<sub>2</sub>O<sub>7</sub>: Eu<sup>2+</sup> phosphor with high Internal Quantum Efficiency and Remarkable Thermal Stability

Vinita Chouhan<sup>1</sup>, Nidhi Malviya<sup>2</sup>, Nazish Khan<sup>3</sup>, Shilpi Rawat<sup>4</sup>

<sup>1,3,4</sup>Assistant professor, Department of Chemistry, UIT, BU, Bhopal, M. P., India

<sup>2</sup>Assistant professor, Department of Science, Government College Rehti, Sehore, M.P., India

## Abstract:

Green-emitting phosphor NaBaScSi<sub>2</sub>O<sub>7</sub>:Eu<sup>2+</sup> was synthesized by “Amorphous Metal Complex” method using water soluble silicon compound. Eu<sup>2+</sup> doped NaBaScSi<sub>2</sub>O<sub>7</sub> exhibited a broad green emission band centered between 500 and 510 nm. The high luminescence intensity of the as-synthesized phosphors may owe to the synthesis procedure based on Amorphous Metal Complex (AMC) method which helps in the homogeneous distribution of Eu<sup>2+</sup> ions in the matrix as well as the double annealing in graphite and H<sub>2</sub>/N<sub>2</sub> reducing atmosphere. Upon excitation at 365 nm, the composition-optimized NaBaScSi<sub>2</sub>O<sub>7</sub>:Eu<sup>2+</sup> exhibited strong green light peaking at 501 nm with the CIE chromaticity (0.146, 0.375) and a high internal quantum efficiency of about 77%. The thermally stable luminescence properties were also studied. The results indicate NaBaScSi<sub>2</sub>O<sub>7</sub>:Eu<sup>2+</sup> as an attractive candidate for use as a conversion phosphor for Phosphor Converted White light-emitting diode (pc-WLEDs) applications.

**Keywords:** LEDs, NBS, WSS, AMC method.

## 1. Introduction

In recent year white light-emitting diodes (LEDs) have been employed in different illumination systems worldwide. An increasing number of traditional illumination devices are being replaced by LEDs. Because of their high brightness, low energy consumption, long lifetime, high efficiency and eco-friendly [1-6]. White light-emitting diodes (LEDs) are applied not only in lighting device but also in extensive fields, such as agriculture lighting, automobile, and backlighting [7-9]. UV-LED chips with red, green, and blue phosphors have attracted considerable attention as next-generation LED devices because of their high color rendering index [10]. The commercial green phosphor for White light-emitting diodes can be mainly classified as nitrides/oxynitrides represented by SiAlON:Eu<sup>2+</sup> and Si<sub>2</sub>Si<sub>2</sub>O<sub>2</sub>N<sub>2</sub>:Eu<sup>2+</sup> and silicates represented by Ca<sub>3</sub>Sc<sub>2</sub>Si<sub>3</sub>O<sub>12</sub>:Ce<sup>3+</sup> and Ba<sub>2</sub>SiO<sub>4</sub>:Eu<sup>2+</sup> [11-12]. However, there are some disadvantages for the presently used this phosphors. A well-known defect is that the synthesis of nitride phosphors needs a critical condition, such as high temperature and high pressure of N<sub>2</sub> [13].

There are some silicates phosphors have been reported. Generally have lower thermal stability. Therefore, it is essential to explore new green-emitting phosphors for *near*-UV pumped LEDs. For example,  $\text{MYSi}_4\text{N}_7$  ( $M = \text{Sr, Ba}$ ) [14],  $\text{MSi}_2\text{O}_2\text{N}_2$  ( $M = \text{Ca, Sr, Ba}$ ) [15],  $\text{M}_3\text{Si}_6\text{O}_{12}\text{N}_2$  ( $M = \text{Sr, Ba}$ ) [16],  $\beta\text{-SiAlON}$  [17-18], rankinite ( $\text{Ca}_3\text{Si}_2\text{O}_7$ ) [19], jervisite ( $\text{NaScSi}_2\text{O}_6$ ) [20], wastromite ( $\text{BaCa}_2\text{Si}_3\text{O}_9$ ) [21], akermanite ( $\text{Ca}_2\text{MgSi}_2\text{O}_7$ ) [22], anorthite ( $\text{CaAl}_2\text{Si}_2\text{O}_8$ ) [23] or pyrope ( $\text{Mg}_3\text{Al}_2(\text{SiO}_4)_3$ ) [24] doped with a rare-earth ion, can act as an efficient phosphor. The large number of phosphors derived from minerals evidences the fact that this “mineral inspired methodology” for developing a new phosphor is advantageous and less time-consuming than the combinational method developed by a generic algorithm [25].

White light emitting diode present in the market are phosphor-converted LEDs (pc-LEDs) constituted by a blue InGaN chip and a yellow phosphor,  $(\text{Y,Gd})_3(\text{Al,Ga})_5\text{O}_{12}:\text{Ce}^{3+}$  (YAG: $\text{Ce}^{3+}$ ) [26]. Although this type of white LEDs has been widely used for many years, they are limited to a high correlated color temperature (CCT; usually, 6000 K) and a low color rendering index (CRI; usually, 75) [27–30], which restricts their use in more colorful applications. In order to obtain higher efficiency white LEDs with appropriate CCT and higher CRI, more scientific efforts have been therefore focused on using near-ultraviolet (n-UV) or ultraviolet (UV) LED chips coated with blue/green/red tricolor phosphors [31,32]. N-UV pc-LEDs have many potential applications as a result of their excellent CRI, high color tolerance, and high conversion efficiency to visible light [33]. Currently, many illumination applications require significantly higher brightness levels than indicator applications, which have motivated the development of high-power n-UV LEDs [34]. Thus, one of the major challenges for n-UV LEDs is delivering the highest efficiency performance at the high current densities and temperatures relevant to high-power operation. As a result, new phosphors with high efficiency and good thermal stability are desperately needed because the white light generated by pc-LEDs with a UV/n-UV LED chip strongly depends on the phosphor stability [35–37]. Therefore, there is an urgent demand to develop new n-UV/UV excitable phosphors with high efficiency and excellent thermal stability. Moreover, as a promising technology in flat panel displays, field emission.

The discovery of green-emitting phosphors with high luminescence intensity has attracted an increasing research interest. In exploration of new White light-emitting phosphor we adopt a “mineral inspired methodology”. The silicates are good candidates to serve as the host structure due to several merits such as excellent chemical and thermal stability and their abundance in nature. The development of high-efficiency phosphors with various colors is one of the most important issues that need to be addressed to improve the performance of white LEDs.  $\text{Eu}^{2+}$  activated phosphors are most suited to obtain emissions of various colors (from the blue to the red region), because the emission resulting from the  $4f^65d^1 - 4f^7$  electronic transition is strongly correlated with the energy gap between  $5d$  and  $4f$  orbitals, which are strongly affected by both the nephelauxetic and crystal field effects of  $\text{Eu}^{2+}$  ions [38].

We consider two key points for the appearance of high efficiency phosphor emissions owing to the  $4f^65d^1 - 4f^7$  electronic transitions of the  $\text{Eu}^{2+}$  activators in the phosphors, which are (i) the selection of the appropriate host compounds and (ii) the uniform dispersion of  $\text{Eu}^{2+}$  activators in the host compounds. In the case of the former, silicon-based oxides and nitrides [39-41] aluminates [42] and sulphides [43-44] are the most appropriate host compounds for such high-efficiency phosphors. Among them, oxide-based compounds are the most promising candidates for high-efficiency phosphors because of their good performance and productivities.

Host selection is an important factor in this development process. For the exploration of a new phosphor we adopt a “mineral inspired methodology”. Among different possible matrices, silicates are good

candidates to serve as the host structure due to several merits such as excellent chemical and thermal stability and high efficiency their abundance in nature.

S. ray *et al.* reported the silicate phosphors using an aqueous solution parallel synthesis method with propylene glycol-modified silane (PGMS). NaBaScSi<sub>2</sub>O<sub>7</sub> (NBS) phosphors, that exhibits a broad excitation spectrum in the near-ultraviolet-to-violet range and emits intense blue light at 365 nm excitation, we report the temperature dependent luminescence behavior of Eu<sup>2+</sup> doped prepared through Amorphous metal complex process by using PGMS as silicate source for the first time, also with an aim to develop new phosphor used for white LEDs, we have studied the luminescence properties of Eu<sup>2+</sup> was introduced into the NaBaScSi<sub>2</sub>O<sub>7</sub> host in the reducing atmosphere, and the special crystallographic positions of the Eu<sup>2+</sup> were determined based on XRD, crystal structure, photoluminescence study and thermal stability of NaBaScSi<sub>2</sub>O<sub>7</sub>:Eu<sup>2+</sup> successfully analyzed. Thermal stability of phosphor becomes very important to develop new kinds of phosphor materials. Nowadays, the pc-white LEDs have been developed with higher power where the chips release high temperatures (e.g., in the range of 100 °C - 150 °C). The temperature is one out of several factors that determine the quality of LEDs such as color coordinates, etc. So, understanding the luminescence behavior against temperature is important and necessary to improve the optical performance of pc-LEDs etc.

## 2. Experimental

NaBaScSi<sub>2</sub>O<sub>7</sub>:Eu<sup>2+</sup> has been synthesized with the help of “Amorphous Metal Complex” method using water soluble silicon compound. In a typical synthesis, Sodium Carbonate (NaCO<sub>3</sub>), Barium Carbonate (BaCO<sub>3</sub>) dissolved in citric acid solutions, Scandium Nitrate [Sc(NO<sub>3</sub>)<sub>3</sub>] and Europium Nitrate [Eu(NO<sub>3</sub>)<sub>3</sub>] solutions have been used. “Propylene glycol modified silane” (PGMS), which has been used as a source of Si, was obtained by an alkoxy group exchange reaction with tetra hydroxy silane (TEOS) in the presence of an acid as a catalyst. For the synthesis of PGMS, 0.4 mol of PG (Kanto Chemical 99.9%) and 0.1 mol of TEOS (Kanto Chemical, 99.9%) were transferred by a digital pipette into a 100 ml conical flask with a stopper. Due to the insolubility of TEOS in PG, the liquid mixture was divided into two phases. 100 ml of concentrated hydrochloric acid (HCl, Kanto Chemical, 36%) was added as a catalyst for the alkoxy group exchange reaction. The mixture was stirred in a magnetic stirrer at 80 °C for 1 h which resulted in the formation of a transparent uniform solution without any phase separation. This solution can be mixed with water in any ratio without hydrolysis of the silicon compound. This compound is named as PGMS. The solution was then transferred from conical flask into a 100 ml volumetric flask and diluted with distilled water to obtain a 1M PGMS solution. The AMC method includes different steps like poly-esterification at 130 °C for 6 h followed by several heat treatment steps at 450 °C, 550 °C and 800 °C to obtain the precursor. Finally the precursor was heat treated at 1150 °C for 3 h under H<sub>2</sub>/N<sub>2</sub> atm.

In this process, required amount of NaCO<sub>3</sub> and BaCO<sub>3</sub> salts are dissolved in an aqueous solution of citric acid. Then desired amount of Sc (NO<sub>3</sub>)<sub>3</sub> and Eu (NO<sub>3</sub>)<sub>3</sub> solutions are added to it. The temperature of the solution has been increased to 80 °C and kept for 2 h. Then the temperature has been increased gradually to 130 °C followed by the addition of required amount of WSS solution. After complete evaporation of the solution a transparent gel has been formed. Then the gel has been subjected to pyrolysis at 450 °C for 12 h and then heat treated at 550 °C for 4 h and 800 °C for 5 h for obtaining the precursor. Finally, the precursor has been annealed in the presence of H<sub>2</sub>/N<sub>2</sub> atmosphere at 1150 °C for 3 h to get the required sample. The formation process also shows in figure.

It is noteworthy that the uniform distribution of activator ions into the host matrix is the key factor responsible for the enhancement of luminescence intensity of the phosphor. In this context, the above-mentioned 'AMC' method has several advantages as follows:

1. Complexation of the cations by citric acid greatly improved the stability of the initial solution against hydrolysis or precipitation, which increases the local activator concentration and eventually diminishes the emission intensity of the phosphor.
2. The dissolution of Scandium Oxide ( $\text{Sc}_2\text{O}_3$ ) in nitric acid was difficult and, for the first time we have reported the synthesis of  $[\text{Sc}(\text{NO}_3)_3]$  by the prolonged heat treatment (about 7 days) of  $\text{Sc}_2\text{O}_3$  in concentrated  $\text{HNO}_3$  aqueous solution at  $80^\circ\text{C}$  under constant stirring condition.
3. The water evaporation generates the formation of a gel with high viscosity, in which, the mobility of the metal ions get lowered [45] which in turn is responsible for the prohibition of the undesirable segregation of metal ions. It is important to mention that an aqueous solution of PGMS solution undergoes self-gelation and solidify if the hydrolysis of PGMS proceeds very slowly [46].

To get the improved uniformity of the dopants ion into the matrix, self-gelation of PGMS is detrimental as it would increase the local activator concentration. In AMC method, after the addition of PGMS, two competitive gelation processes takes place simultaneously, reaction of PGMS with metal-citrate precursor along with self-gelation of PGMS. It has been reported that the hydrolysis of PGMS proceeds quickly with the enhancement of temperature, which in turn decreases the self-gelation of PGMS. For this reason, the temperature of the hot plate was raised to  $130^\circ\text{C}$  to suppress the self-gelation process at the expense of reaction of PGMS with metal-citrate precursor.

## 2.1 Characterization

The phase purity of the as-synthesized sample was identified by using powder X-ray diffraction (XRD) analysis with a Bruker AXS D8 advanced automatic diffractometer with Cu-K $\alpha$  radiation ( $\lambda = 1.5418 \text{ \AA}$ ), over the angular range  $10^\circ \leq 2\theta \leq 80^\circ$ , operating at 40 kV and 40 mA. Structural refinements to the XRD patterns were made using the Full Prof Suite program (version 2.05) [47]. The photoluminescence (PL) excitation and emission spectra of the samples were analyzed by using a RF-5301PC (Shimadzu, Japan) equipped with a 150 W Xenon light source and the slit width was kept 1.5 nm. The temperature dependent PL spectra were obtained with a spectrophotometer (Jobin-Yvon Spex, Model FluoroMax-3). The CIE chromaticity coordinates were plotted using Radiant Imaging colour calculator software.

## 3 Results and Discussions

### 3.1 Crystal Structure and X-ray Diffraction (XRD) Analysis

Material Characterization: The XRD measurements were carried out using Bruker D8 Advance X-ray were produced using a sealed tube and the wavelength of X-ray was 0.154 nm (Cu K-alpha). The X-ray was detected using a fast counting detector based on silicon trip technology (Bruker LynxEye detector). For all the rare earth doped phosphors, the powders were pressed in the middle of the sample holder to make a flat surface before put into the scanning chamber. All data were collected from  $10^\circ$  to  $60^\circ$  ( $2\theta$ ) for 35 minutes in the step scan mode. In figure 2 the XRD of  $\text{NaBaScSi}_2\text{O}_7:\text{Eu}^{2+}$  phosphor with stoichiometric Na and with 10%, 20%,

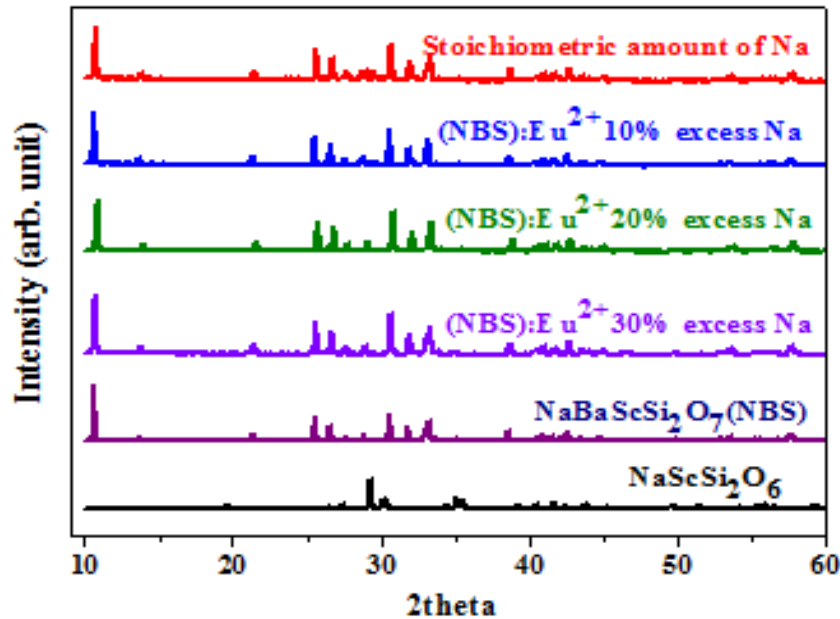


**Figure 1 XRD of NBS: Eu<sup>2+</sup> Samples synthesized in the presence of stoichiometric amount of Na, 10%, 20% and 30% excess Na.**

30% excess Na with respect its stoichiometric requirement. The 100% pure phase is obtained with adding 30% excess amount of Na.

Figure 2 show the proportion of impurity (NaScSi<sub>2</sub>O<sub>6</sub>) is negligible by increasing H<sub>2</sub> reduction time. In order to understand the phase purity of the as-prepared NaBaScSi<sub>2</sub>O<sub>7</sub>:Eu<sup>2+</sup> phosphor, the X-ray diffraction data was implemented of NaBaScSi<sub>2</sub>O<sub>7</sub>:Eu<sup>2+</sup> phosphor and it is inferred that the phosphor has crystallized in a single phase [47]. NaBaScSi<sub>2</sub>O<sub>7</sub>:Eu<sup>2+</sup> crystallizes in a monoclinic unit cell with the space group *P*2<sub>1</sub>/*n*, similar to the one reported for pure NaBaScSi<sub>2</sub>O<sub>7</sub> host [48]. The substitution of Eu<sup>2+</sup> ions in the Ba site led to a slight variation in the lattice parameters and the volume of the unit cell. The ionic radii of Ba<sup>2+</sup> being slightly greater than Eu<sup>2+</sup>, no major issues incurred with the substitution of Ba<sup>2+</sup> site with Eu<sup>2+</sup> ions. This was also achieved without disturbing the charge balance of the phosphor system. The monoclinic structure bears only one site each for Na, Ba and Sc. Ba site being most favourable in terms of ionic radii and charge neutrality, Eu<sup>2+</sup> ions have replaced some Ba<sup>2+</sup> ions in the host lattice.

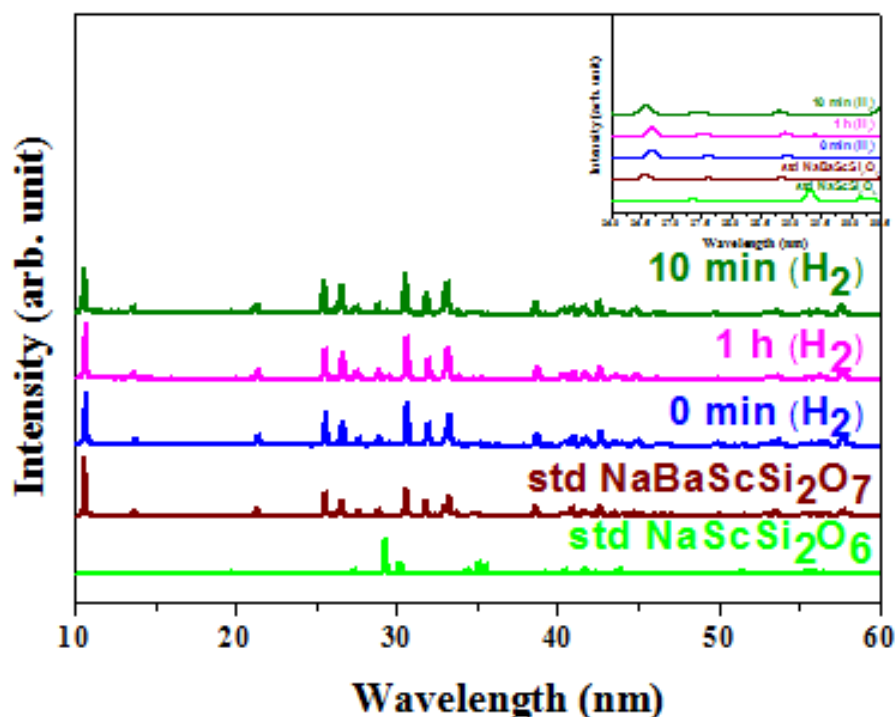


Figure 2 XRD patterns of NaBaScSi<sub>2</sub>O<sub>7</sub> with different H<sub>2</sub> reduction time.

### 3.2 Crystal structure of NaBaScSi<sub>2</sub>O<sub>7</sub>

In 2010, the ring silicate structure of host lattice NaBaScSi<sub>2</sub>O<sub>7</sub> (NBS) has been reported for the first time by Maria et. al. The disilicate NaBaScSi<sub>2</sub>O<sub>7</sub> forms monoclinic crystals with space-group symmetry *P21/m*, with *a* 6.845(1), *b* 5.626(1), *c* 8.819(2) Å,  $\beta$  109.33(3)°, *V* 320.47(10) Å<sup>3</sup>, *Z* = 2. The asymmetric unit of NaBaScSi<sub>2</sub>O<sub>7</sub> contains one Ba, one Na, one Sc, two Si and five O atoms. Atoms Na, Sc, Si(1), Si(2), O(2), O(3) and O(4) are located on mirror planes, *y* = ½, and Ba on *y* = ¾, whereas the two remaining O atoms are in general positions. The Ba atom is coordinated by nine oxygen atoms with an average Ba–O bond length of 2.87 Å. The Na atom is eight-coordinated with a mean Na–O bond length of 2.74 Å. The average Sc–O bond length amounts to 2.10 Å, which is nearly identical to the average Sc–O value, 2.105 Å, reported by Baur (1981). The Si(1)- and Si(2)-centered SiO<sub>4</sub> tetrahedra are slightly distorted, with mean Si–O bond lengths of 1.62 and 1.63 Å, and O–Si–O angles of 106.42 and 112.21°. The versatile structure of NaBaScSi<sub>2</sub>O<sub>7</sub> offers three types of sites for the occupancy of various cations, type I with trivalent Sc sites in ScO<sub>6</sub> polyhedra; type II with divalent Ba sites in BaO<sub>9</sub> polyhedra and type III with mono-valent Na sites having 8-fold coordination. In this structure, the existing different types of sites are available for the occupancy of guest cations with different charges. In the present work, the ionic radii of Sc<sup>3+</sup>, Ba<sup>2+</sup> and Na<sup>+</sup> are 0.74, 1.47 and 1.18 Å, and the ionic radii for the six-, eight- and nine coordinated Eu<sup>2+</sup> are 1.17, 1.25 and 1.30 Å.<sup>16</sup> Therefore, based on the comparison of the effective ionic radii of cations with different coordination numbers, it could offer the possible opportunity for Eu<sup>2+</sup> doping ions to enter into the Sc<sup>3+</sup>, Ba<sup>2+</sup> and Na<sup>+</sup> ion sites, and the detailed analysis of the crystallographic occupancy is given below Figure [48].

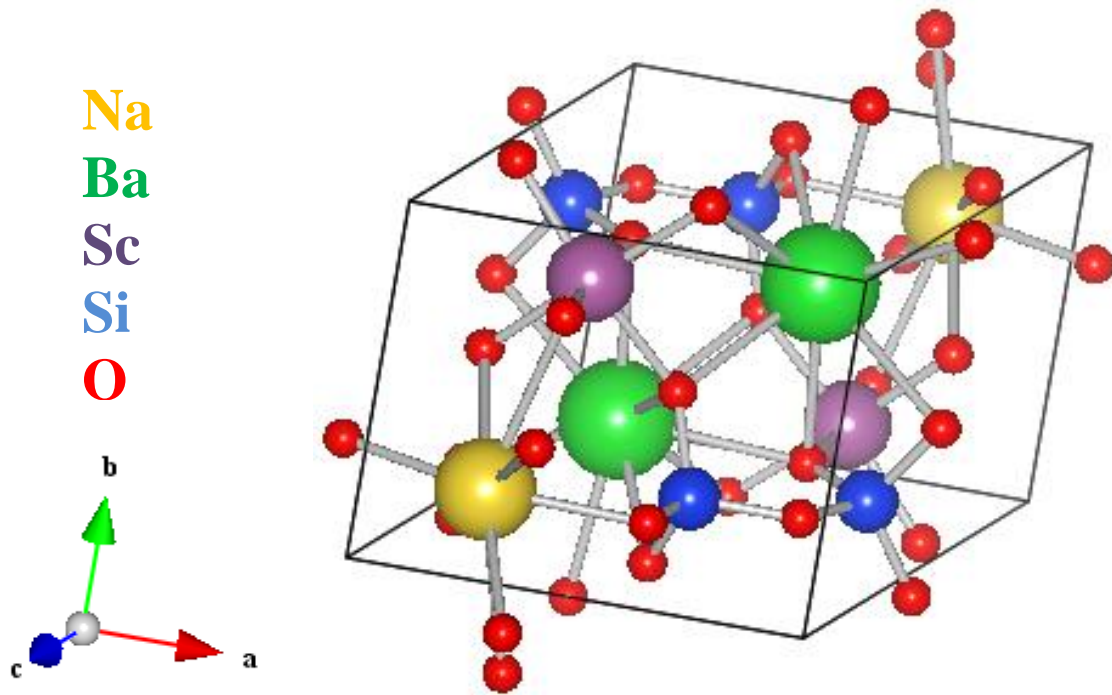


Figure 3 Crystal Structure of NaBaScSi<sub>2</sub>O<sub>7</sub>

### 3.3 Photoluminescence Study

The luminescence spectrum of NBS:Eu<sup>2+</sup> obtained with 365 nm excitation at room temperature exhibited an intense green emitting band with the maxima at 500 nm. The corresponding excitation spectrum exhibited strong absorption at 365 nm (excitation maxima), green light was weakly absorbed by the due to the <sup>4</sup>f<sup>7</sup>→<sup>4</sup>f<sub>6</sub><sup>5</sup>d<sub>1</sub> transitions of Eu<sup>2+</sup> ions, matches well with the wavelengths emitted by commercial near-UV LED chips (360-400 nm).

To understand the PL intensity with the concentration of doped Eu<sup>2+</sup> ions in

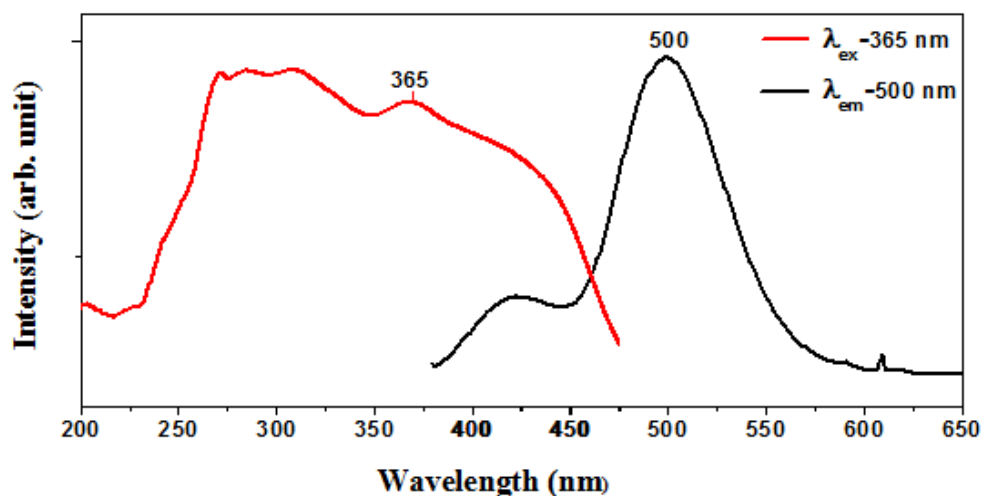


Figure 4 PLE and PL spectra of NaBaScSi<sub>2</sub>O<sub>7</sub>:Eu<sup>2+</sup>

NaBaScSi<sub>2</sub>O<sub>7</sub> phosphor, a NaBaScSi<sub>2</sub>O<sub>7</sub>:Eu<sup>2+</sup> (Eu<sup>2+</sup> = 0.2 mol) phosphors were synthesized. The PL emission spectra for 2 mol % concentrations of Eu<sup>2+</sup> ions doped in NaBaScSi<sub>2</sub>O<sub>7</sub> phosphor, excited at 365 nm wavelengths, are shown in Fig. 4. The PL intensity is found to increase from 0.2 mol% of the dopant concentration until the concentration is 2 mol% and this is the optimum concentration value wherein maximum PL intensity is observed. There is a decrease observed in the intensity for concentrations greater than 2 mol% of Eu<sup>2+</sup> ions. It is noteworthy to mention that excitation spectra of NBS:Eu<sup>2+</sup> appears quite different from the one reported by Chiu et al [49].

### 3.4 Thermal stability

Thermal stability of a phosphor is a crucial technological parameter for pc-LEDs because the surface temperature of the current driven LED chips on which the phosphors are mounted is around 120 °C. The thermal quenching temperature (T50) is defined as the temperature at which the PL intensity is 50% of its original value. Temperature-dependent PL spectra of NBS:Eu<sup>2+</sup> measured at 25-300 °C under excitation at 356 nm is shown in Fig.6. Interestingly, the PL intensity of NBS:Eu<sup>2+</sup> is 95% retained at 150 °C of that measured at room temperature [Fig. 6] which is almost comparable than that of commercial BAM:Eu<sup>2+</sup> (91.3%) as presented in inset of . It is noteworthy that with the increase in the temperature, the population density of phonons is increased, and the electron-phonon interaction is dominant, which results in broadening of the emission spectra. These are common features that occur as a result of the temperature dependence of the electron-phonon interactions in the ground and excited states of the luminescence centers [50].

As shown in Fig.5 at 300 °C, NBS:Eu<sup>2+</sup> retains 70.69% with respect to its room temperature emission intensity, which indicates that T50 of this compound is above 300 °C. It is noteworthy that with the increase in the temperature, the population density of phonons is increased, and the electron-phonon interaction is dominant, which results in broadening the emission spectra [50].

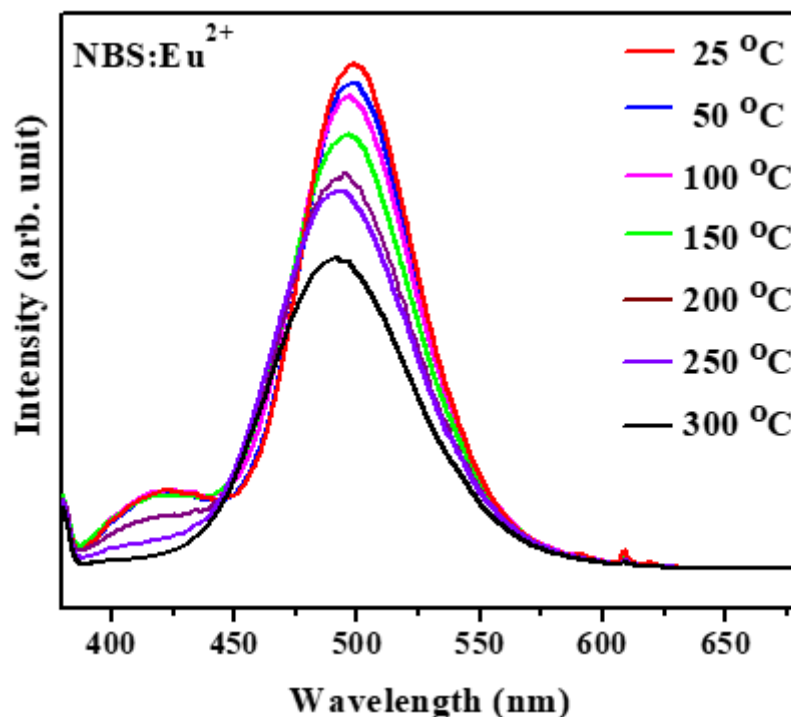


Figure 5 Temperature-dependent PL spectra of NaBaScSi<sub>2</sub>O<sub>7</sub>:Eu<sup>2+</sup>.



#### 4 Conclusions

In this paper, we described the synthesis parameter, which have been adopted for the optimization of the phase purity, involved in the exploration of new phosphors using the AMC method based on a mineral-inspired approach by using of propylene glycol-modified silane (PGMS). We present the successful development of a green emitting phosphor, NBS:Eu<sup>2+</sup> for phosphor converted white light emitting diodes (W-LEDs), by a solution based approach. The phase analysis of the phosphor by powder XRD along with the room temperature as well as high temperature PL study have been carried out. It has been observed that the phosphor can be efficiently excited by 365 nm near-UV light and emit green emission centered at about 501 nm. High Temperature PL study of NBS: Eu<sup>2+</sup> phosphor reflects its excellent thermal stability with the retention of 77% of its room temperature PL intensity at 150 °C. All these observations reflect the potential of the phosphor for the application in pc-LED.

#### References

1. Wang, L., Wang, X., Kohsei, T., Yoshimura, K. i., Izumi, M., Hirosaki, N., Xie, R. J., *Opt. Express*, 23, 28707 (2015).
2. Yeh, C. W., Chen, W. T., Liu, R. S., Hu, S. F., Sheu, H. S., Chen, J. M., Hintzen, H. T., *J. Am. Chem. Soc.*, 134, 14108 (2012).
3. Chen, W. T., Sheu, H. S., Liu, R. S., Attfield, J. P., *J. Am. Chem. Soc.*, 134, 8022 (2012).
4. Daicho, H., Iwasaki, T., Enomoto, K., Sasaki, Y., Maeno, Y., Shinomiya, Y., Aoyagi, S., Nishibori, E., Sakata, M., Sawa, H., Matsuishi, S., Hosono, H., *Nat Commun*, 3, 1132 (2012).
5. Xie, R. J., Hirosaki, N., *Sci. Technol. Adv. Mater.*, 8, 588 (2007).
6. Hoppe, H. A., *Angew. Chem. Int. Ed*, 48, 3572 (2009).
7. Vogel, S. J., *Oxford. Econ Pap*, 136 (1994).
8. Su, S. J.; Chen, X. X.; Shi, W. B.; Zhu, W. T., *J. Semicond. Technol, Sci*, 8, 007 (2007).
9. Wei, L. L., Lin, C. C. Fang, M. H., Brik, M. G., Hu, S. F., Jiao, H., Liu, R. S., *A Low- J. Mater. Chem. C*, 3, 1655 (2015).
10. Sheu, J. K. Chang, S. J. Kuo, C. Su, Y. K.; Wu, L. Lin, Y. Lai, W. Tsai, J. Chi, G. C. Wu, R., *Photonics Technol. Lett*, 15, 18 (2003).
11. Bachmann, V., Ronda, C., Oeckler, O., Schnick, W., Meijerink, A. *Chem. Mater*, 21, 316 (2009).
12. Shimomura, Y., Honma, T., Shigeiwa, M., Akai, T., Okamoto, K., Kijima, N. *J. Electrochem. Soc.*, 154, 35 (2007).
13. Schnick, W., Huppertz, H., Lauterbach, R. *J. Mater. Chem*, 9, 289 (1999).
14. Kurushima T, Gundiah G, Shimomura Y, et al. *J. Electrochem. Soc.*, 157, 64 (2010).
15. Botterman J, Van den Eeckhout K, Bos A J J, et al. *Opt. Mater. Express*, 2, 341 (2012).
16. Song Y H, Choi T Y, Senthil K, et al. *Mater. Lett*, 65, 3399 (2011).
17. Hirosaki N, Xie R J, Kimoto K, et al. *Appl. Phys. Lett*, 86, 211905 (2005).
18. Xie R J, Hirosaki N, Li H L, et al. *J. Electrochem. Soc.*, 154, 314 (2007).
19. F. Qian, R. Fu, S. Agathopoulos, X. Gu and X. Song, *J. Lumin*, 132, 71 (2012).
20. S. Merlino and P. Orlandi, *Period Mineral*, 75, 189 (2006).
21. S. Yao, L. Xue and Y. Yan, *Opt. Laser Technol*, 43, 1282 (2011).
22. L. Jiang, C. Chang, D. Mao and C. Feng, *Opt. Mater*, 27, 51 (2004).
23. J. K. Park, J. M. Kim, E. S. Oh and C. H. Kim, *Electrochem. Solid-State Lett*, 8, H6 (2005).
24. T. Ohagaki, A. Higashida, K. Soga and A. Yasumori, *J. Electrochem. Soc.*, 154, J163 (2007).

25. A. K. Sharma, C. Kulshreshtha and K. S. Sohn, *Adv. Funct. Mater*, 19, 1705 (2009).
26. H. A. Höppe, *Angew. Chem*, 121, 3626 (2009).
27. A. A. Setlur, *Electrochem. Soc. Interface*, 18, 32 (2009).
28. M. Roushan, X. Zhang and J. Li, *Angew. Chem*, 124, 451 (2012).
29. M. Roushan, X. Zhang and J. Li, *Angew. Chem, Int. Ed.* 51, 436 (2012).
30. A. A. Setlur, W. J. Heward, Y. Gao, A. M. Srivastava, R. G. Chandran and M. V. Shankar, *Chem. Mater*, 18, 3314 (2006).
31. S. E. Brinkley, N. Pfaff, K. A. Denault, Z. Zhang, H. T. Hintzen, R. Seshadri, S. Nakamura and S. P. DenBaars, *Appl. Phys. Lett*, 99, 241106 (2011).
32. Y. Uchida and T. Taguchi, *Opt. Eng.*, 2005, 44, 124003 and C. C. Lin, Z. R. Xiao, G. Y. Guo, T. S. Chan and R. S. Liu, *J. Am. Chem. Soc*, 132, 3020 (2010).
33. E. Radkov, R. Bompiedi, A. M. Srivastava, A. A. Setlur and C. Becker, *Proc. SPIE*, 5187, 171 (2004).
34. M. H. Crawford, *IEEE J. Sel. Top. Quantum Electron*, 15, 1028 (2009).
35. W. B. Im, N. N. Fellows, S. P. DenBaars and R. Seshadri, *J. Mater. Chem*, 19, 1325 (2009).
36. Y. C. Yang and S. L. Wang, *J. Am. Chem. Soc*, 130, 1146 (2008).
37. Ki and J. Li, *J. Am. Chem. Soc*, 130, 8114 (2008).
38. P. Dorenbos, *J. Lumin*, 104, 239 (2003).
39. G. Blasse and A. Bril: *J. Solid State Chem*, 2, 105 (1970).
40. R.-J. Xie, N. Hirosaki, T. Suehiro, F.-F. Xu, and M. Mitomo, *Chem. Mater*, 18, 5578 (2006).
41. K. Uheda, N. Hirosaki, Y. Yamamoto, A. Naito, T. Nakajima, and H. Yamamoto, *Electrochem. Solid-State Lett*, 9, H22 (2006).
42. S. H. M. Poort, W. P. Blokpoel, and G. Blasse, *Chem. Mater*, 7, 1547 (1995).
43. Y. Hu, W. Zhuang, H. Ye, S. Zhang, Y. Fang, and X. Huang *J. Lumin*, 111, 139 (2005).
44. P. F. Smet, K. Korthout, J. E. Van Haecke, and D. Poelman, *Mater. Sci. Eng. B*, 146, 264 (2008).
45. Marsh, P. J., Silver, J., Vecht, A., Newport, A. *J. Lumin*, 97, 229 (2002).
46. Yoshizawa, K., Kato, H., Kakihana, M. *J. Mater. Chem*, 22, 17272 (2012).
47. Rodríguez-Carvajal, J. *Phys. B Condens. Matter*, 192, 55 (1993).
48. Maria Wierzbicka-Wieczorek, M.; Uwe, K.; Tillmanns, E. *Can. Mineral*, 48, 51 (2010).
49. Abe, T., Woog, S., Ishigaki, T., Uematsu, K., Toda, K., Sato, M. *J. Ceram. Process. Res*, 15, 181 (2014).
50. Kim, J. S., Park, Y. H., Kim, S. M., Choi, J. C., Park, H. L. *Solid State Commun*, 133, 445 (2005).